Polyhydride (Fluoroalkyl)phosphine Complexes of Iridium. Synthesis, Dynamics, and Reactivity Properties of $(dfepe)_2Ir_2(\mu\text{-}H)_3(H)$

R. Chris Schnabel, Patrick S. Carroll, and Dean M. Roddick*

Department of Chemistry, Box 3838, University of Wyoming, Laramie, Wyoming 82071

Received September 8, 1995[⊗]

The synthesis and reactivity properties of new dimeric iridium polyhydrides incorporating the acceptor ligand $(C_2F_5)_2PCH_2CH_2(C_2F_5)_2$ (dfepe) are reported. Hydrogenolysis of (dfepe)Ir(η^3-C_3H_5) (prepared by metathesis of [(dfepe)Ir(μ-Cl)]$_2$ with allylmagnesium chloride) afforded $(dfepe)_2Ir_2(\mu\text{-}H)_3(H)$ (**3**) in high yield as an air-stable red crystalline solid. A triply bridged ground-state geometry for **3** was deduced from low-temperature NMR data and was confirmed by X-ray crystallography. Hydride site exchange mechanisms are proposed which are consistent with VT ^1H and ^{31}P NMR data. Although **3** is formally coordinatively saturated, hydride bridge dissociation readily occurs and leads to ligand addition reactions. Thus, treatment of tetrahydride **3** with 1 atm of H_2 at 20 °C quantitatively affords the hexahydride dimer [(dfepe)Ir(μ-H)$_2$(H)$_2$]$_2$ (**5**). In the absence of H_2, **5** rapidly loses H_2 in solution at 20 °C to re-form **3**. The structure of **5** has been determined by X-ray crystallography. **3** also reacts with CO to give (dfepe)Ir(CO)$_2$H (**6**), which loses CO under 1 atm of H_2 to reversibly afford (dfepe)Ir(CO)H$_3$ (**7**). The trihydride undergoes thermal H/D exchange with both D_2 (20 °C) and benzene-d_6 (120 °C), presumably via the intermediacy of (dfepe)Ir(CO)H. The tetrahydride **3** also undergoes H/D exchange with D_2 and benzene-d_6 under similar conditions. In the presence of *tert*-butylethylene, dehydrogenation of cyclopentane by **3** at 120 °C quantitatively affords CpIr(dfepe); a likely intermediate in this process is the dihydride dimer [(dfepe)Ir(μ-H)]$_2$. (dfepe)Ir(η^3-C_3H_5) also reacts directly with cyclopentane at 120 °C to give CpIr(dfepe).

Downloaded by CARLI CONSORTIUM on June 30, 2009
Published on January 23, 1996 on http://pubs.acs.org | doi: 10.1021/om950722c

Introduction

Polynuclear hydride complexes of the cobalt triad are of longstanding interest and continue to be an attractive target in synthetic inorganic chemistry. Depending on the steric and electronic properties of the ancillary phosphine, phosphine hydride complexes [$(R_3P)_2$Rh(H)]$_2$[1−5] and $(R_3P)_4M_2(H)_4$ (M = Co,[7] Rh[4−6]) as well as higher nuclearity products [$(R_3P)_2$Rh(H)]$_n$ (n = 3, 4)[1,5b] have been characterized. Although both polynuclear cobalt and rhodium phosphine hydride systems and their reactions with small molecules have been extensively studied, the corresponding chemistry of iridium remains relatively undeveloped. To date, the chemistry of iridium phosphine hydrides has been primarily limited to higher valent Ir(III) and Ir(V) monomeric $(R_3P)_3IrH_3$[8] and $(R_3P)_2IrH_5$[9,10] systems as well as cationic Ir(III) dimers.[11−13]

We have recently reported the synthesis of both monomeric and binuclear hydride complexes of iridium which incorporate the strongly electron-withdrawing (perfluoroalkyl)phosphine chelate $(C_2F_5)_2PCH_2CH_2P(C_2F_5)_2$ ("dfepe").[14] Of particular significance was the isolation and structural characterization of a novel mixed-valent Ir(I)−Ir(III) trihydride dimer, $(dfepe)_2Ir_2(H)(\mu\text{-}H)_2(\mu\text{-}O_3SCF_3)$. Although this compound may be viewed as the protonolysis product of [(dfepe)Ir(μ-H)]$_2$, attempts to prepare this compound via deprotonation of $(dfepe)_2Ir_2(H)(\mu\text{-}H)_2(\mu\text{-}O_3SCF_3)$ were unsuccessful due to the high apparent reactivity of the parent Ir(I) hydride dimer. These results, together with the notable absence of iridium analogues to cobalt and rhodium $(R_3P)_4Rh_2(H)_2$ and $(R_3P)_4M_2(H)_4$ donor phosphine systems, have prompted us to examine alternative synthetic routes to low-valent (dfepe)Ir(H)$_x$ systems. Accordingly, we have initiated a general study of structural and reactivity properties of (fluoroalkyl)phosphine polyhydride complexes of iridium.

⊗ Abstract published in *Advance ACS Abstracts,* December 15, 1995.

(1) Sivak, A. J.; Muetterties, E. L. *J. Am. Chem. Soc.* **1979**, *101*, 4878.
(2) Meier, E. B.; Burch, R. R.; Muetterties, E. L.; Day, V. W. *J. Am. Chem. Soc.* **1982**, *104*, 2661.
(3) Teller, R. G.; Williams, J. M.; Koetzle, T. F.; Burch, R. R.; Gavin, R. M.; Muetterties, E. L. *Inorg. Chem.* **1981**, *20*, 1806.
(4) Fryzuk, M. D.; Piers, W. E.; Einstein, F. W. B.; Jones, T. *Can. J. Chem.* **1989**, *67*, 883.
(5) (a) Fryzuk, M. D. *Can. J. Chem.* **1983**, *61*, 1347. (b) Fryzuk, M. D. *Organometallics* **1982**, *1*, 408.
(6) Thorn, D. L.; Ibers, J. A. *Adv. Chem. Ser.* **1982**, *No. 196*, 117.
(7) Fryzuk, M. D.; Ng, J. B.; Rettig, S. J.; Huffman, J. C.; Jonas, K. *Inorg. Chem.* **1991**, *30*, 2437.
(8) Ahmad, N.; Robinson, S. D.; Uttley, M. F. *J. Chem. Soc., Dalton Trans.* **1972**, 843.
(9) (a) Werner, H.; Höhn, A.; Schulz, M. *J. Chem. Soc., Dalton Trans.* **1991**, 777. (b) Goldman, A. S.; Halpern, J. *J. Organomet. Chem.* **1990**, *382*, 237. (c) Faller, J. W.; Smart, C. J. *Organometallics* **1989**, *8*, 602. (d) Cameron, C. J.; Felkin, H.; Fillebeen-Khan, T.; Forrow, N. J.; Guittet, E. *J. Chem. Soc., Chem. Commun.* **1986**, 801. (e) Crabtree, R. H.; Lavin, M. *J. Chem. Soc., Chem. Commun.* **1985**, 1661. (f) Empsall, H. D.; Hyde, E. M.; Mentzer, E.; Shaw, B. L.; Uttley, M. F. *J. Chem. Soc., Dalton Trans.* **1976**, 2069. (g) Mann, B. E.; Masters, C.; Shaw, B. L. *J. Inorg. Nucl. Chem.* **1971**, *33*, 2195.
(10) Clerici, M. G.; di Gioacchino, S.; Maspero, F.; Perrotti, E.; Zanobi, A. *J. Organomet. Chem.* **1975**, *84*, 379.
(11) (a) Wang, H. H.; Pignolet, L. H. *Inorg. Chem.* **1980**, *19*, 1470. (b) Crabtree, R. H.; Felkin, H.; Morris, G. E. *J. Organomet. Chem.* **1977**, *141*, 205.
(12) El-Amouri, H.; Bouayad, A. *Polyhedron* **1989**, *8*, 1945.
(13) Bianchini, C.; Farnetti, E.; Graziani, M.; Kaspar, J.; Vizza, F. *J. Am. Chem. Soc.* **1993**, *115*, 1753.
(14) Schnabel, R. C.; Roddick, D. M. *Organometallics* **1993**, *12*, 704.

0276-7333/96/2315-0655$12.00/0 © 1996 American Chemical Society

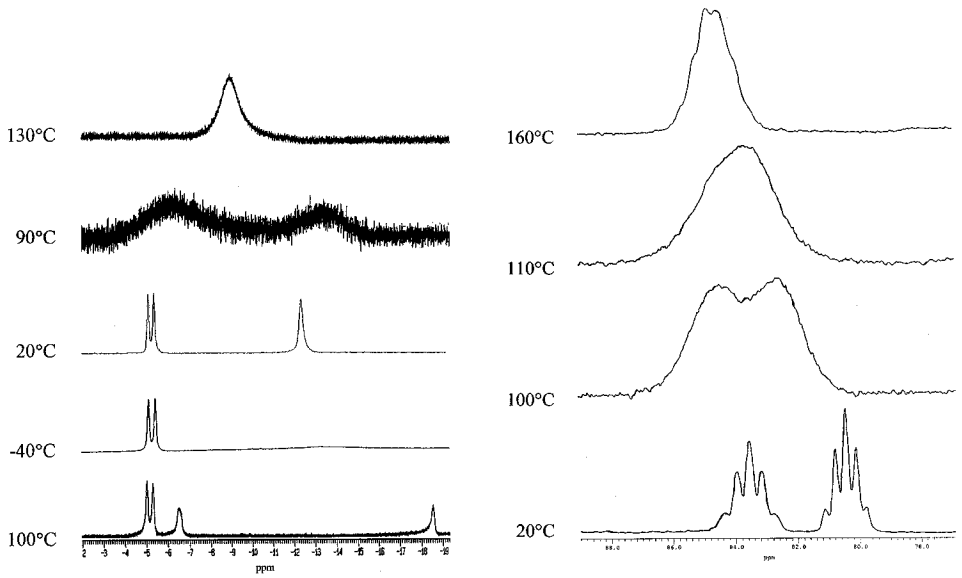

Figure 1. Variable-temperature ^{1}H (left) and ^{31}P (right) NMR spectra of (dfepe)$_2$Ir$_2$(μ-H)$_3$H (**3**). Ambient- and subambient-temperature proton spectra were taken in acetone-d_6; higher temperature proton spectra were taken in toluene-d_8. ^{31}P NMR spectra were taken in mesitylene.

Downloaded by CARLI CONSORTIUM on June 30, 2009
Published on January 23, 1996 on http://pubs.acs.org | doi: 10.1021/om950722c

Results and Discussion

Synthesis of (dfepe)M(π-C$_3$H$_5$) (M = Rh, Ir) and (dfepe)$_2$Ir$_2$(μ-H)$_3$(H). A well-precedented route to cobalt and rhodium phosphine hyride complexes of the general form [(R$_3$P)$_n$M(H)$_m$]$_x$ is via hydrogenolysis of the corresponding allyl compounds, (R$_3$P)$_n$M(π-C$_3$H$_5$) (n = 2, 3). The previously reported chloro dimers [(dfepe)-M(μ-Cl)]$_2$ (M = Rh, Ir)[15] provide an effective entry to the desired allyl systems. Treatment of these chloro dimers with allylmagnesium chloride gave the allyl complexes (dfepe)M(π-C$_3$H$_5$) (M = Rh (**1**), Ir (**2**)) as readily sublimable crystalline solids in high yield (eq 1).

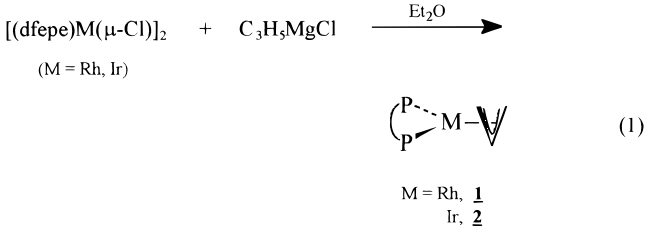

(1)

The ^{1}H NMR spectral data for both **1** and **2** are similar to those reported for analogous (Ph$_3$P)$_2$M(π-C$_3$H$_5$) systems.[1,10,16] In addition to the resonances of the dfepe ligand, the anti allyl protons of **1** appear at δ 2.25 as a doublet of doublets due to coupling with the central allyl proton ($^3J_{HH}$ = 14 Hz) and a single phosphorus atom ($^3J_{PH}$ = 8 Hz). The syn protons appear as a broad doublet at δ 4.48 ($^3J_{HH}$ = 8 Hz). Coupling between the syn and anti protons is not resolved. In addition to coupling with both the syn and anti protons, the central allyl proton resonance for **1** is also coupled to rhodium ($^2J_{RhH}$ = 4 Hz). The ^{1}H NMR spectrum of **2** is similar to that of **1**, except that the central allyl proton exhibits a triplet fine structure due to virtual coupling with both phosphorus nuclei. The ^{31}P NMR spectra for both **1** and **2** consist of single, broad, highly fluorine coupled resonances ($^1J_{PRh}$ = 226 Hz for **1**). In accord with earlier (R$_3$P)$_2$M(π-allyl) studies, these complexes are formulated as mononuclear square-planar derivatives with the allyl ligand formally occupying two cis coordination sites. Both **1** and **2** are air-stable in the solid state. In contrast to the triphenylphosphine complex (Ph$_3$P)$_2$Ir(π-C$_3$H$_5$), which is reported to have limited solution stability at room temperature, solutions of **2** in benzene exhibit no decomposition after several days at 120 °C.

The hydrogenolysis of a hexane solution of (dfepe)-Rh(π-C$_3$H$_5$) under 2 atm of H$_2$ proceeded quite slowly over the course of several days at ambient temperature to give an uncharacterized and thermally unstable insoluble dark green solid. In contrast, treating (dfepe)-Ir(π-C$_3$H$_5$) with 1 atm of H$_2$ at room temperature rapidly evolved propane and afforded the air-stable red binuclear tetrahydride (dfepe)$_2$Ir$_2$(H)$_4$ (**3**) in high yield (eq 2). This result differs from the hydrogenolysis of (R$_3$P)$_2$-

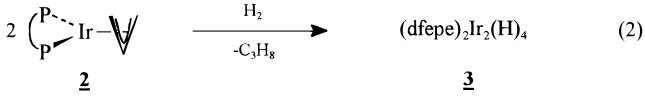

(2)

Ir(π-allyl) complexes, which has been to reported to give only the pentahydride products (R$_3$P)$_2$IrH$_5$.[16a] Complex **3** is remarkably stable to both air and moisture and may be heated to 100 °C in water-saturated toluene under air for several hours without significant decomposition.

The room-temperature ^{1}H NMR spectrum of **3** shows hydride resonances at δ −4.69 (br d, $^2J_{HP}$ = 119 Hz) and −12.53 (br s) of equal intensity; these chemical shift values are characteristic of bridging and terminal hydride coordination, respectively. Two phosphorus resonances are observed at δ 83.9 and 80.8. Although these data are consistent with the static Ir(III)−Ir(I) unsymmetrical dimer formulation (dfepe)(H)$_2$Ir(μ-H)$_2$Ir-(dfepe), low-temperature ^{1}H NMR (acetone-d_6, 400 MHz) data for **3** indicate the triply bridged ground-state structure (dfepe)$_2$Ir$_2$(H)(μ-H)$_3$, which undergoes rapid exchange of the terminal hydride ligand with a unique

(15) Schnabel, R. C.; Roddick, D. M. *Inorg. Chem.* **1993**, *32*, 1513.
(16) (a) Schulz, M.; Werner, H. *J. Organomet. Chem.* **1994**, *470*, 243. (b) Fryzuk, M. D. *Inorg. Chem.* **1982**, *21*, 2134. (c) Reilly, C. A.; Thyret, H. *J. Am. Chem. Soc.* **1967**, *89*, 5144.

Downloaded by CARLI CONSORTIUM on June 30, 2009
Published on January 23, 1996 on http://pubs.acs.org | doi: 10.1021/om950722c

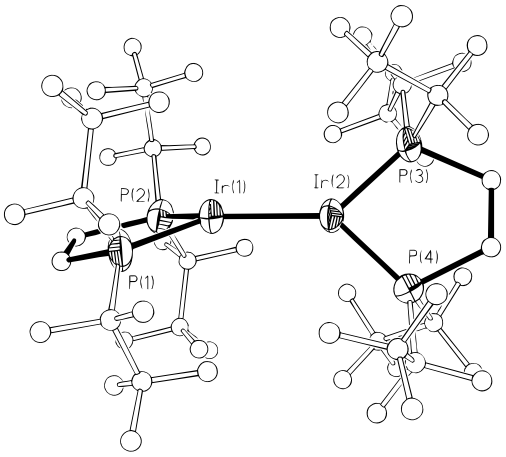

Figure 2. Molecular structure of $(dfepe)_2Ir_2(\mu\text{-}H)_3H$ (**3**) with atom-labeling scheme (30% probability ellipsoids).

trans bridging hydride. As shown in Figure 1, the resonance at δ −4.69 ascribed to the two equivalent bridging hydride ligands remains unchanged down to −100 °C. However, coalescence of the terminal hydride resonance at δ −12.53 was observed at −50 °C. A slow-exchange limit was reached at −100 °C which showed unique bridging and terminal hydride resonances at δ −6.39 and −18.71. Analogous behavior has been reported previously for $(R_3P)_4M_2(H)_4$ systems.[1,4] The activation free energy for this exchange between the terminal and unique bridging hydride ligand is $\Delta G^{\ddagger} = 8.8(4)$ kcal mol^{-1}, a value which is essentially identical with that reported for $[(^iPrO)_3P]_4Rh_2(H)_4$ (∼9 kcal mol^{-1})[1] and the propylene-bridged phosphine chelate system $(dippp)_2Rh_2(H)_4$ (8.6(5) kcal mol^{-1})[4] and somewhat greater than that found for $(dippe)_2Rh_2(H)_4$ (<7.0-(5) kcal mol^{-1}), which has an ethylene-bridged phosphine chelate. Although dynamic ^{1}H NMR data for the dippe chelate system are consistent with ground-state geometries **A** and **B**, X-ray data for **3** reveal the

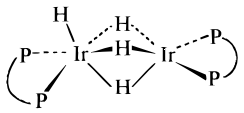

A

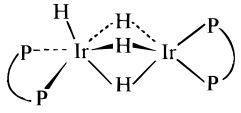

B

staggered chelate ring ground state geometry **B** (Figure 2), similar to that of the structurally characterized $[(^iPrO)_3P]_4Rh_2(H)_4$. Crystallographic data and selected bond distances and angles for **3** are given in Tables 1 and 2. The precision of the metrical data was limited due to perfluoroethyl and chelate backbone disorder (see Experimental Section); nevertheless, the observed Ir−Ir distance of 2.536(3) Å is comparable with those of other iridium triply bridged hydride systems such as $[(dppp)_2Ir_2H_5]^+$ (2.514(1) Å)[11a] and $[(Ph_3P)_4Ir_2H_5]^+$ (2.52 Å).[11b] The dihedral angle between the planes defined by Ir(1), P(2), P(2) and Ir(2), P(3), P(4) in **3** is 79.9°, which is very similar to the corresponding value of 72.6° reported for $[(^iPrO)_3P]_4Rh_2(H)_4$. Only two ^{31}P NMR signals are observed for **3** down to −100 °C, rather than three signals as expected for geometry **B**. However, substantial broadening of the upfield phosphorus resonance takes place between −80 and −100 °C, suggesting that the slow-exchange limit for the nonisochronous phosphorus nuclei of the five-coordinate iridium center occurs at $T < -100$ °C.

Table 1. Crystallographic Data for $(dfepe)_2Ir_2(\mu\text{-}H)_3H$ (3) and $[(dfepe)Ir(\mu\text{-}H)H_2]_2$ (5)

	$(dfepe)_2Ir_2(\mu\text{-}H)_3H$	$[(dfepe)Ir(\mu\text{-}H)H_2]_2$
	Crystal Data	
chem formula	$C_{20}H_{12}F_{40}Ir_2P_4$	$C_{20}H_{14}F_{40}Ir_2P_4$
fw	1520.6	1522.6
cryst syst	monoclinic	orthorhombic
color	red	yellow
space group	$P2_1/n$ (No. 14)	*Pbca* (No. 61)
size (mm)	0.20 × 0.32 × 0.82	0.20 × 0.40 × 0.50
a (Å)	17.576(4)	15.531(3)
b (Å)	12.308(2)	11.613(2)
c (Å)	19.327(4)	21.287(4)
β (deg)	110.06(3)	
V (Å^3)	3927.3(14)	3839.4(12)
Z	4	4
T (°C)	−100	−100
λ (Å)	0.710 73	0.710 73
D_{calc} (g cm^{-3})	2.572	2.634
μ (cm^{-1})	71.44	72.74
T(max)/T(min)		5.64
	Data Collection	
scan method	Wyckoff	Wyckoff
scan limits (deg)	4−50	4−55
data collected (h,k,l)	+20,+14,±22	+20,+15,−27
no. of rflns collected	7144	4407
no. of indpndt rflns	6903	4407
obsd rflns	3041 ($F_o > 4\sigma(F_o)$)	2278 ($F_o > 4\sigma(F_o)$)
	Refinement	
$R(F)$ (%)	12.10	7.16
$R(wF)$ (%)	15.18	7.31
GOF	3.07	1.56
Δ/σ(max)	0.03	0.10
$\Delta(\rho)$ (e Å^{-3})	2.42	3.88
N_o/N_v	12.6	7.4

[a] $R(F_o) = \sum(|F_o| - |F_c|)/\sum|F_o|$; $R_w(F_o) = \sum(w^{1/2}(|F_o| - |F_c|))/\sum(w^{1/2}|F_o|)$, $w^{-1} = \sigma^2(F_o) + 0.0008(F_o)^2$.

Table 2. Selected Bond Lengths (Å) and Angles (deg) for $(dfepe)_2Ir_2(\mu\text{-}H)_3H$ (3) and $[(dfepe)Ir(\mu\text{-}H)H_2]_2$ (5)[a]

	$(dfepe)_2Ir_2(\mu\text{-}H)_3H$	$[(dfepe)Ir(\mu\text{-}H)H_2]_2$
	Bond Distances	
Ir(1)−Ir(1a)		2.703(2)
Ir(1)−Ir(2)	2.536(3)	
Ir(1)−P(1)	2.20(1)	2.198(5)
Ir(1)−P(2)	2.21(1)	2.296(5)
Ir(2)−P(3)	2.19(1)	
Ir(2)−P(4)	2.20(1)	
	Bond Angles	
Ir(2)−Ir(1)−P(1)	139.2(4)	
Ir(2)−Ir(1)−P(2)	130.1(4)	
P(1)−Ir(1)−P(2)	87.4(5)	85.1(2)
P(3)−Ir(2)−P(4)	85.7(5)	
Ir(1)−Ir(2)−P(3)	137.4(4)	
Ir(1)−Ir(2)−P(4)	135.9(3)	
Ir(1a)−Ir(1)−P(1)		145.3(2)
Ir(1a)−Ir(1)−P(2)		105.4(1)
	Torsional Angles	
P(1)−Ir(1)−Ir(2)−P(3)	−126.3	
P(1)−Ir(1)−Ir(2)−P(4)	69.2	
P(2)−Ir(1)−Ir(2)−P(3)	81.5	
P(2)−Ir(1)−Ir(2)−P(4)	−83.0	
P(1)−Ir(1)−Ir(1a)−P(2a)	76.0	

[a] Metrical data are given for the primary iridium position, Ir(1). Metrical data for the secondary iridium position Ir(2) are given in the Supporting Information.

The limited stability of $(R_3P)_4Rh_2(H)_4$ systems with respect to H_2 loss precludes the study of hydride fluxionality at higher temperatures. In contrast, $(dfepe)_2Ir_2(H)(\mu\text{-}H)_3$ is thermally stable in the absence of dihydrogen and affords us the opportunity to examine higher energy intramolecular hydride exchange pro-

Scheme 1

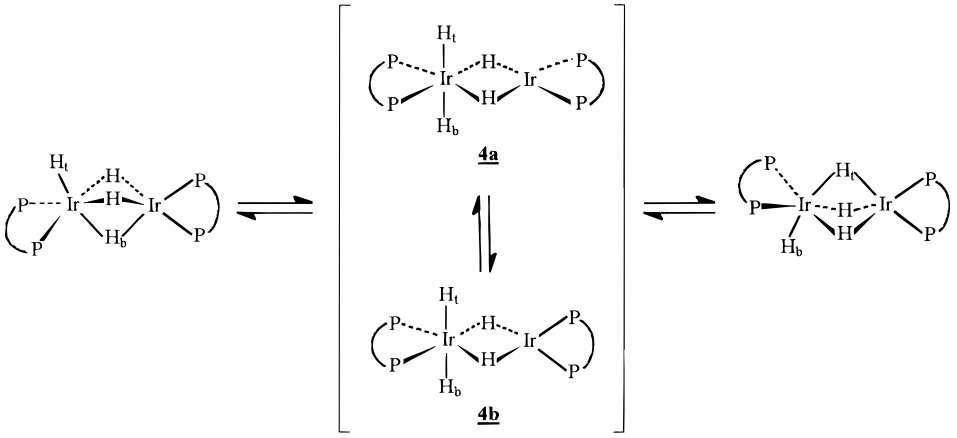

Scheme 2

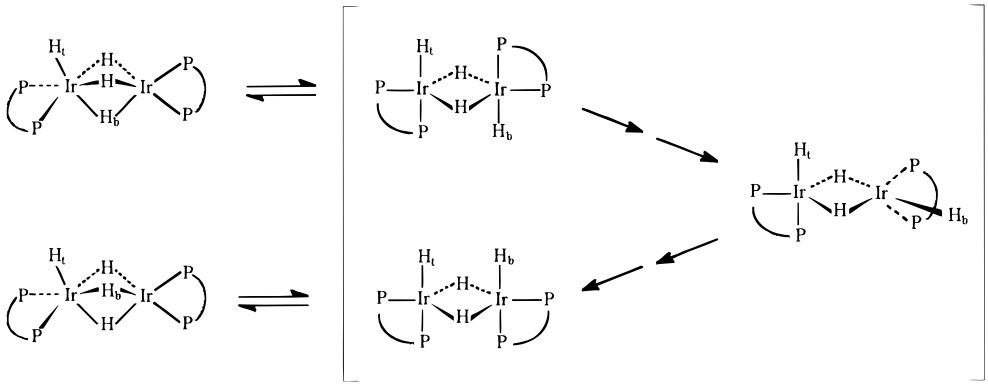

Downloaded by CARLI CONSORTIUM on June 30, 2009
Published on January 23, 1996 on http://pubs.acs.org | doi: 10.1021/om950722c

cesses involving the remaining bridging hydride positions. At 70 °C (toluene-d_8, 270 MHz), both the terminal and hydride resonances appear as broad singlets (Figure 1). Further warming results in coalescence at 100 °C, corresponding to an activation free energy of $\Delta G^{\ddagger} = 15.7(4)$ kcal mol^{-1}; a single broad hydride resonance is observed at 150 °C in this solvent. High-temperature ^{31}P NMR spectra of **3** (mesitylene, 161.7 MHz) are complicated by extensive fluorine coupling and temperature-dependent chemical shifts. Nevertheless, coalescence is observed at approximately 110 °C, which corresponds to a $\Delta G^{\ddagger}$ value for phosphorus site exchange of 17(1) kcal mol^{-1}.[17] The free energy values for hydride and phosphorus site exchange are similar and suggest a common exchange mechanism.

Two closely related mechanisms for the exchange of the terminal hydride and a unique bridging hydride in complexes with the ground-state structure **B** have been previously considered (Scheme 1). For the monodentate phosphite complex $[(^{i}PrO)_3P]_4Rh_2(H)_4$, Muetterties initially proposed a permutation of the terminal hydride and a unique bridging hydride involving intermediate **4a**, with trans terminal hydride ligands and a square-planar Rh(I) center.[1] For a closely related dippp chelate system, Fryzuk proposed the intermediate geometry **4b** with a tetrahedral Rh(I) center, although **4a** was not ruled out.[4] Although **4b** is attractive from a least-motions standpoint, SCF calculations for intramolecular hydride exchange in $(H_3P)_4Rh_2(H)_4$ indicate that the activation barrier between **4a** and **4b** is low and that **4a** is energetically preferred.[18] Observation of two distinct phosphorus resonances under the conditions of low-temperature hydride exchange rules out the additional possibility of a symmetrical intermediate, $[(dfepe)Ir(H)(\mu\text{-}H)]_2$.

At least one additional exchange mechanism involving the unique $Ir_2(\mu\text{-}H)_2$ core must be invoked to explain the equilibration of all the hydride and phosphorus environments in **3** at higher temperatures. Since both hydride sets are stereochemically distinguished by the six-coordinate Ir(III) center in **4**, unbridging either the unique bridging hydride or one of the other bridging hydride ligands to form an unsymmetrical intermediate with fluxional trigonal-bipyramidal iridium centers is necessary. Pseudorotation followed by hydride rebridging on the opposite $Ir_2(\mu\text{-}H)_2$ face results in exchange of all hydride positions (Scheme 2). Alternatively, exchange of hydride sites may also be accomplished by dissociating a bridging hydride in **4a** or **4b** to give an intermediate with six- and three-coordinate iridium centers, which may freely rotate about the remaining Ir(μ-H)Ir bridge. This mechanism does not account for equilibration of the phosphorus sites, however.

Synthesis and Characterization of [(dfepe)Ir(H)$_2$(μ-H)]$_2$ (5). The energetic accessibility of coordinatively unsaturated four-coordinate Ir(I) intermediates such as **4a** and **4b** inferred by dynamic NMR studies is lent further support by the reactivity of the tetrahydride dimer with additional dihydrogen. Exposure of a hex-

(17) The uncertainty assigned to $\Delta G^{\ddagger}$ for phosphorus site exchange is estimated by assigning a maximum $\Delta\nu$ value of 1000 Hz. This assumes that the monotonic upfield shift of ν_{av} for the two ^{31}P signals between 25 and 110 °C is entirely due to the upfield phosphorus resonance.

(18) Branchadell, V.; Dedieu, A. *New J. Chem.* **1988**, *12*, 443.

Downloaded by CARLI CONSORTIUM on June 30, 2009
Published on January 23, 1996 on http://pubs.acs.org | doi: 10.1021/om950722c

ane slurry of **3** to H_2 (2 atm) at ambient temperature results in the quantitative precipitation after 24 h of the yellow hexahydride dimer **5** (eq 3). Rapid loss of H_2 and regeneration of **3** upon dissolution in acetone or other coordinating solvents made the spectroscopic characterization of **5** difficult. However, NMR samples of **3** sealed under 3 atm of H_2 in acetone-d_6 show approximately a 66% conversion to **5** at 25 °C. ^{1}H NMR spectra under these conditions show hydride resonances at δ −7.09 (br d, $^2J_{HP}$ = 149 Hz) and −21.90 (br s) which are integrated as four and two protons, respectively. A single ^{31}P multiplet is observed at δ 84.3. Although a static trans terminal hydride structure is consistent with these data, the solid-state structure of **5** (see below) reveals a cis hydride geometry. The low-temperature solution dynamics of **5** could not be investigated due to solubility limitations. The H_2 addition/elimination equilibrium shown in eq 3 provides a facile pathway for

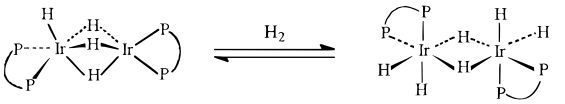

(3)

3 **5**

deuterium incorporation into **3**, since the symmetrical hexahydride **5** can undergo elimination from either iridium center. In accord with this expectation, treatment of **3** with 2 atm of D_2 at 20 °C leads to complete isotopic scrambling into both terminal and bridging hydride sites after 2 h. A decrease (∼30%) in the integrated intensity of the terminal/unique bridging hydride resonance at −12.53 ppm relative to the remaining bridging hydride resonance during the early stages of deuterium exchange is consistent with terminal hydride isotopic scrambling with D_2 prior to intramolecular hydride site exchange (Scheme 2).

The solid-state structure of **5** has been determined by X-ray diffraction at −100 °C; selected data collection and material data are presented in Tables 1 and 2. **5** is essentially isomorphous with the previously reported hexahydride dimer $[(Me_2PhP)_2Ir(H)(\mu\text{-}H)]_2$, which also crystallizes in the orthorhombic space group *Pbca* and possesses crystallographically imposed inversion symmetry relating to two iridium centers (Figure 3).[19] A positional disorder between alternative iridium sites (84:16 site occupation ratio) related by approximate 2-fold symmetry and an accompanying disorder in several of the dfepe perfluoroethyl groups (see Experimental Section) reduce the precision of this structure. Nevertheless, several structural features warrant comment. Although the hydride ligands were not located, the orientations of P(1) and P(2) with respect to the Ir(1)−Ir(1a) axis (Ir(1a)−Ir(1)−P(2) = 105.4(1)°; Ir(1a)−Ir(1)−P(1) = 145.3(2)°) are similar to corresponding values for $[(Me_2PhP)_2Ir(H)(\mu\text{-}H)]_2$ (94.9 and 140.4°) and are consistent with the presence of terminal hydrides trans to P(2) and cis to P(1). The greater deviation of Ir(1a)−Ir(1)−P(2) from the ideal value of 90° is due to chelate constraints. The observed Ir−Ir bond distance, 2.703(2) Å, is similar to that of $[(Me_2PhP)_2Ir(H)(\mu\text{-}H)]_2$ (2.739(1) Å). The 0.10 Å lengthening seen in **5** for the Ir−P bond trans to a terminal hydride ligand relative to the Ir−P bond trans to a bridging hydride (2.296(5) versus

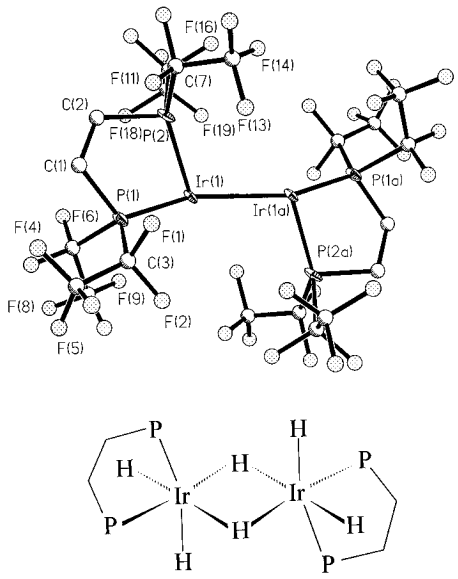

Figure 3. Molecular structure of $[(dfepe)Ir(\mu\text{-}H)H_2]_2$ (**5**) with atom-labeling scheme (30% probability ellipsoids). An illustration of **5** showing the implied hydride ligand positions is given for comparison.

2.198(5) Å) is also comparable to that seen in $[(Me_2PhP)_2Ir(H)(\mu\text{-}H)]_2$ (2.315(2) versus 2.231(3) Å); this substantial trans influence is more consistent with a classical hydride structure rather than an alternative Ir(I) dihydride formulation such as $[(dfepe)Ir(\eta^2\text{-}H_2)(\mu\text{-}H)]_2$.[20]

(dfepe)$_2$Ir$_2$(μ-H)$_3$H Carbonylation Chemistry: Synthesis of (dfepe)Ir(CO)H$_3$ (7). Treatment of benzene solutions of **3** with 1 atm of CO cleanly affords the previously reported dicarbonyl hydride $(dfepe)Ir(CO)_2H$ (**6**) after 2 h at ambient temperature (eq 4).[14] Monitoring

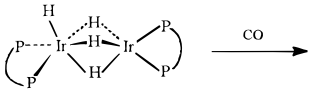

3

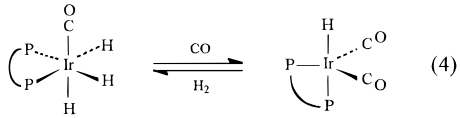

(4)

7 **6**

the reaction between $(dfepe)_2Ir_2(\mu\text{-}H)_3H$ and CO by ^{1}H NMR at early stages of the reaction revealed the buildup of the transient trihydride complex $(dfepe)Ir(CO)H_3$ (**7**); after 30 min, the conversion of **3** to **6** was complete. The trihydride exhibits a broad hydride doublet at δ −8.88 ($^2J_{HP}$(trans) ≈ 146 Hz) and a triplet at δ −12.37 ($^2J_{HP}$(cis) = 22 Hz) in a 2:1 ratio. These hydride coupling patterns are similar to those reported for the donor phosphine complex *fac*-$(dppe)Ir(CO)H_3$ and, together with ^{31}P and ^{19}F NMR data, confirm that **7** also adopts a facial geometry.[21,22] The formation of **6**

(19) Robertson, G. B.; Tucker, P. A. *Aust. J. Chem.* **1984**, *37*, 257.

(20) The normal Ru−Cl bond length in *trans*-$[(dppe)_2Ru(\eta^2\text{-}H_2)Cl]^+$ indicates that the trans influence of η^2-H_2 is quite low: Chin, B.; Lough, A. J.; Morris, R. H.; Schweitzer, C. T.; D'Agostino, C. *Inorg. Chem.* **1994**, *33*, 6278.

(21) Eisenberg, R.; Fisher, B. J. *Organometallics* **1983**, *2*, 764.

(22) The AA′XX′ ^{1}H NMR pattern expected for the equatorial hyrides in *fac*-$(dfepe)Ir(CO)H_3$ simplifies to a broadened doublet due to long-range fluorine coupling.

Scheme 3

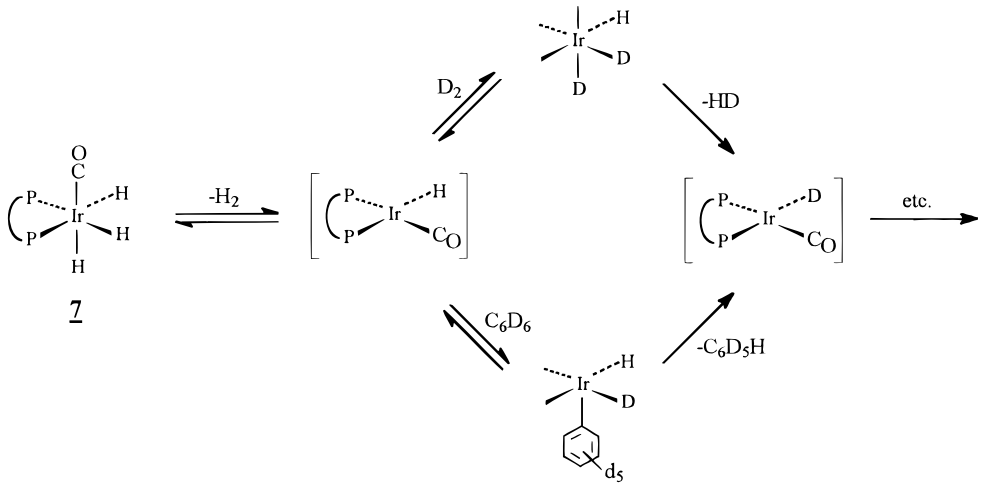

from **7** is reversible: treatment of (dfepe)Ir(CO)$_2$H with 1 atm of H_2 in diethyl ether at 20 °C precipitated (dfepe)-Ir(CO)H_3 as a white solid in high yield. This interconversion between (dfepe)Ir(CO)H_3 and (dfepe)Ir(CO)$_2$H is consistent with the formation of the common 16-electron intermediate (dfepe)Ir(CO)H under mild conditions. For comparison, interconversion between (dppe)-Ir(CO)$_2$H and (dppe)Ir(CO)H_3 has been observed at *ca.* 50−60 °C.[23]

The intermediacy of (dfepe)Ir(CO)H is similarly implicated in deuterium exchange reactions between (dfepe)Ir(CO)H_3 and D_2 or benzene-d_6 (Scheme 3). After 24 h, exchange between 7 and 1 atm of D_2 at 20 °C is 67% complete; no hydride site selectivity is apparent under these conditions. The trihydride is reactive toward aromatic C−H bonds under more forcing conditions: after 24 h at 120 °C, H/D exchange between both hydride ligand sets of **7** and benzene-d_6 solvent was 70% complete (^{1}H NMR). Eisenberg has previously reported both thermal and photochemical exchangee of (dppe)-Ir(CO)H_3 with deuterium gas.[21] Interestingly, H/D exchange with benzene-d_6 to form (dppe)Ir(CO)D_3 was observed only under photochemical conditions; thermal H/D exchange of (dppe)Ir(CO)H_3 with benzene-d_6 does not occur up to its decomposition threshold of *ca.* 90 °C. In light of this difference between H_2 and benzene-d_6 reactivities, an alternative C−H activation mechanism involving photochemical phosphine dissociation to form a reactive (η^1-dppe)IrH_3(CO) was proposed. Although a similar mechanism may be operative for **7**, the direct reaction of aromatic C−H bonds with (dfepe)Ir(CO)H under the more thermally forcing conditions available to **7** is also reasonable.

Alkane Activation Chemistry. The activation of C−H bonds by iridium polyhydrides has been reported in the presence of olefinic hydrogen acceptors.[24] For the pentahydride (^{i}Pr$_3$P)$_2$IrH_5, phosphine metalation[10] as well as hydrocarbon dehydrogenation,[9d] hydrocarbon−olefin coupling,[24] and vinylic H−D exchange[9c] have been observed. In these types of reactions various coordinatively unsaturated iridium species such as (R$_3$P)$_2$IrH_3, (R$_3$P)IrH_3, and (R$_3$P)$_2$IrH have been proposed as reactive intermediates. The addition of dihydrogen to the latent coordination site in tetrahydride **3** to give hexahydride

Scheme 4

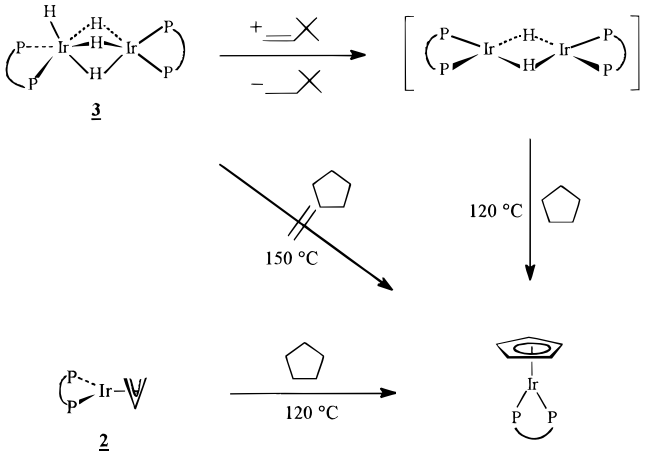

5 (eq 3) suggested that C−H activation might also be possible in this system. Indeed, slow H/D exchange between **3** and benzene-d_6 is observed over the course of several days at 120 °C. This exchange presumably involves arene addition to unsaturated intermediate **4a** or **4b** to give a phenyl-substituted intermediate analogous to **5** (e.g. (dfepe)Ir(Ph)(H)(μ-H)$_2$Ir(H)$_2$(dfepe)).

In contrast to aromatic H/D exchange, no isotopic exchange between **3** and cyclohexane-d_{12} or dehydrogenation of cyclopentane by **3** is detected at temperatures up to 150 °C. In the presence of excess *tert*-butylethylene (5 equiv), however, the clean conversion of **3** in neat cyclopentane to previously reported CpIr(dfepe)[15] is complete after 1 day at 120 °C. A likely active intermediate involved in this process is the coordinatively unsaturated dihydride [(dfepe)Ir(μ-H)]$_2$ (Scheme 4). Interestingly, thermolysis of (dfepe)Ir(η^3-C$_3$H$_5$) in neat cyclopentane also cleanly affords CpIr(dfepe) after 7 days at 120 °C. In this reaction the allyl ligand in (dfepe)Ir(η^3-C$_3$H$_5$) serves as an intramolecular hydrogen acceptor, generating 1 equiv of propane along with the observed cyclopentadienyl product and H_2.

Summary

The hydride chemistry of the (dfepe)Ir moiety differs significantly from that of donor iridium phosphine systems, (R$_3$P)$_2$Ir(H)$_x$, which favor monomeric Ir(V) coordination. Instead, a closer comparison can be made

(23) Eisenberg, R. Personal communication.
(24) Lu, X.; Lin, Y.; Ma, D. *Pure Appl. Chem.* **1988**, *60*, 1299.

Downloaded by CARLI CONSORTIUM on June 30, 2009
Published on January 23, 1996 on http://pubs.acs.org | doi: 10.1021/om950722c

Downloaded by CARLI CONSORTIUM on June 30, 2009
Published on January 23, 1996 on http://pubs.acs.org | doi: 10.1021/om950722c

with rhodium and cobalt systems, which generally prefer M(I) and M(III) oxidation states. Coordinative unsaturation for $(dfepe)_2Ir_2(\mu\text{-}H)_3H$ is readily accessed by hydride unbridging and allows H_2 and CO ligand addition reactions to the four-coordinate iridium center as well as H/D exchange with aromatic C−H bonds. Enhanced reactivity toward aliphatic C−H bonds in the presence of *tert*-butylethylene is attributed to the formation of the dihydride $[(dfepe)Ir(\mu\text{-}H)]_2$ as a reactive intermediate.

The generation of (dfepe)Ir(CO)H under very mild conditions from either CO or H_2 dissociation is an intriguing result, since donor phosphine analogues $(R_3P)_2M(CO)H$ (M = Co, Rh, Ir) are implicated in a wide range of important catalytic processes.[25] (dfepe)Ir(CO)H may thus serve as a useful bridge between electron-rich $(R_3P)_2M(CO)H$ intermediates and metal carbonyl hydrides $(CO)_4MH$ (M = Rh, Ir), which are unstable with respect to cluster formation in the absence of high CO pressures. Furthermore, the high lability of CO observed for $(dfepe)Ir(CO)_2H$ suggests applications in catalytic decarbonylation chemistry and related modes of reactivity where CO inhibition is rate-limiting. We are currently exploring these avenues of research.

Experimental Section

General Procedures. All manipulations were conducted under an atmosphere of nitrogen by using Schlenk, high-vacuum-line, and/or glovebox techniques. Dry, oxygen-free solvents were vacuum-distilled prior to use. Elemental analyses were performed by Desert Analytics. Infrared spectra were recorded on a Mattson Cygnus 100 or Perkin-Elmer 1600 FTIR instrument as Nujol mulls, unless otherwise noted. NMR spectra were obtained by a JEOL JMN-FX270 or GSX-400 instrument. ^{19}F spectra were referenced to CF_3CO_2Et as an internal standard (−75.32 ppm vs $CFCl_3$ with downfield chemical shifts taken to be positive). ^{31}P spectra were referenced to a 85% H_3PO_4 external standard. $[(dfepe)M(\mu\text{-}Cl)]_2$ starting materials were prepared as described previously.[15]

(dfepe)Rh(η^3-C_3H_5) (1). To a solution of $[(dfepe)Rh(\mu\text{-}Cl)]_2$ (0.610 g, 0.433 mmol) in 20 mL of THF at −78 °C was added a THF solution of allylmagnesium chloride (0.50 mL, 2.0 M) dropwise via syringe. The solution turned dark red upon addition and then gradually became light yellow. After 2 h the solvent was quickly removed and the residue was extracted repeatedly with dichloromethane. Reduction of the filtrate to *ca*. 2 mL and cooling to −78 °C yielded 0.540 (86%) of bright yellow crystalline **1**. *NOTE*: (dfepe)Rh(η^3-C_3H_5) readily sublimes at 20 °C (10^{-3} Torr), and care must be taken to avoid product loss during workup under vacuum. Anal. Calcd for $C_{13}H_9F_{20}P_2Rh$: C, 22.00; H, 1.28. Found: C, 22.11; H, 1.28. IR (cm^{-1}): 1632 (w, br), 1416 (w), 1308 (s), 1216 (vs), 1140 (s), 1123 (s), 1084 (m), 962 (s), 916 (w), 807 (w), 748 (w). ^1H NMR (benzene-d_6, 400 MHz, 20 °C): δ 4.71 (ttd, $^3J(H_{anti})$ = 14 Hz, $^3J(H_{syn})$ = 7 Hz, $^2J_{RhH}$ = 3 Hz, 1H; CH_2CHCH_2), 4.48 (*d*, $^3J_{HH}$ = 7 Hz, 2H; syn allyl protons), 2.25 (dd, $^3J_{HH}$ = 14 Hz, $^3J_{PH}$ = 8 Hz, 2H; anti allyl protons), 1.75 (m, 4H; PCH_2). ^{31}P NMR (benzene-d_6, 161.7 MHz, 20 °C): δ 87.4 (dm, $^1J_{RhP}$ = 226 Hz). ^{19}F NMR (benzene-d_6, 376.05 MHz, 20 °C): δ −79.9, −80.3 (s, PCF_2CF_3), −113 to −117.5 (overlapping ABX multiplets, PCF_2CF_3).

(dfepe)Ir(η^3-C_3H_5) (2). To a solution of $[(dfepe)Ir(\mu\text{-}Cl)]_2$ (0.501 g, 0.315 mmol) in 20 mL of diethyl ether at −78 °C was added allylmagnesium chloride (0.36 mL, 2.0 M in THF) dropwise via syringe. The reaction mixture was warmed slowly to ambient temperature and stirred for 12 h, during which time the solution became dark orange. The volatiles were quickly removed, and the residue was sublimed at 50 °C at 10^{-3} Torr onto a water-cooled probe, yielding 0.372 g (74%) of orange crystalline **2**. Anal. Calcd for $C_{13}H_9F_{20}IrP_2$: C, 19.52; H, 1.13. Found: C, 19.48; H, 1.13. IR (cm^{-1}): 1307 (s), 1225 (vs), 1209 (vs), 1142 (s), 1124 (s), 1092 (m), 965 (s), 930 (w), 808 (w), 749 (w). ^1H NMR ($CDCl_3$, 400 MHz, 20 °C): δ 5.07 (ttt, $^3J(H_{anti})$ = 13 Hz, $^3J(H_{syn})$ = 8 Hz, $^3J_{PH}$ = 2 Hz, 1H; CH_2CHCH_2), 4.89 (dt, $^3J_{HH}$ = 8 Hz, $^3J_{PH}$ = 2 Hz, 2H; syn allyl protons), 2.56 (dd, $^3J_{HH}$ = 13 Hz, $^3J_{PH}$ = 4 Hz, 2H; anti allyl protons), 2.20 (m, 4H; PCH_2). ^{31}P NMR (benzene-d_6, 161.7 MHz, 20 °C): δ 81.0 (m). ^{19}F NMR (benzene-d_6, 376.05 MHz, 20 °C): δ −79.8, −80.0 (s, PCF_2CF_3), −114 to −118.5 (overlapping ABX multiplets, PCF_2CF_3).

$(dfepe)_2Ir_2(\mu\text{-}H)_3H$ (3). **2** (0.252 g, 0.315 mmol) was dissolved in 15 mL of diethyl ether, and 1 atm of H_2 was introduced into the system at ambient temperature. Initially orange, the solution turned deep red upon the addition of hydrogen. After the mixture was stirred for 12 h, the solvent volume was reduced to 2 mL, the solution was cooled to −78 °C, and 0.229 g (96%) of red crystalline **3** was collected by cold filtration. Anal. Calcd for $C_{20}H_{12}F_{40}Ir_2P_4$: C, 15.78; H, 0.78. Found: C, 15.56; H, 0.74. IR (cm^{-1}): 2173 (w, br), 1306 (s), 1225 (vs), 1141 (vs), 968 (s), 876 (w), 805 (w), 751 (m). ^1H NMR (benzene-d_6, 269.7 MHz, 20 °C): δ 1.68 (m, 4H, PCH_2), 1.47 (m, 4H, PCH_2), −4.69 (br d, $^2J_{HP}$ = 119 Hz, 2H; Ir(μ-*H*)), −12.53 (br s, 2H, Ir(*H*)). ^{31}P NMR (benzene-d_6, 161.7 MHz, 20 °C): δ 83.9 (m), 80.8 (m). ^{19}F NMR (benzene-d_6, 376.05 MHz, 20 °C): δ −78.5, −79.1 (s, PCF_2CF_3), −112 to −118 (overlapping ABX multiplets, PCF_2CF_3).

$[(dfepe)Ir(\mu\text{-}H)(H)_2]_2$ (5). A Carius tube fitted with a Teflon valve (Chemglass) was charged with 0.502 g of **3** (0.330 mmol), 10 mL of cyclohexane, and *ca*. 3 atm of H_2, and the solution was stirred at ambient temperature for 24 h. During this time, light yellow crystalline **5** precipitated from the initially homogeneous red solution. The solid was collected by filtration, washed several times with cyclohexane, and dried under vacuum. The isolated yield of **5** was 0.488 g (97%). Anal. Calcd for $C_{20}F_{40}H_{14}Ir_2P_4$: C, 15.77; H, 0.92. Found: C, 15.80; H, 0.75. IR (cm^{-1}): 2159 (w, br), 1304 (s), 1225 (vs), 1145 (s), 1125 (s), 1111 (sh), 1084 (m), 963 (s), 861 (m), 808 (w), 748 (m). ^1H NMR (acetone-d_6, 269.7 MHz, 25 °C, under 3 atm of H_2): δ 2.95 (m, 8H, PCH_2), −7.09 (br d, $^2J_{HP}$ = 149 Hz, 4H; Ir(*H*)), −21.90 (br s, 2H, Ir(*H*)). ^{31}P NMR (acetone-d_6, 161.7 MHz, 20 °C): δ 84.3 (m).

Reaction of 3 with CO. The reaction of **3** with 1 atm of CO was monitored by ^1H and ^{31}P NMR spectroscopy in benzene-d_6. After 30 min, resonances for **3** were completely replaced by resonances assignable to the previously reported dicarbonyl hydride, $(dfepe)Ir(CO)_2H$ (**6**).[14] Removal of the volatiles yielded **6** as a yellow oil, 95% pure by ^1H NMR.

***fac*-(dfepe)Ir(CO)H_3 (7).** **3** (0.500 g, 0.329 mmol) in 20 mL of diethyl ether was placed under 1 atm of CO, generating the dicarbonyl **6** *in situ*. After the mixture was stirred for 1 h, the solvent and CO were removed and the residue was redissolved in 2 mL of ether and stirred under 1 atm of H_2 for 1 day. The solvent and H_2 were removed, and the hydrogenation procedure was repeated three times in order to drive off CO and completely convert **6** to **7**. During this time, **7** precipitated from the yellow solution as a white solid. Filtration and washing with cold ether to remove traces of **6** afforded 0.375 g (72%) of **7**. Anal. Calcd for $C_{11}H_7F_{20}IrOP_2$: C, 16.74; H, 0.89. Found: C, 16.80; H, 0.88. IR (cm^{-1}): 2123 (m, br), 2011 (s), 1298 (s), 1218 (vs), 1133 (s), 1085 (m), 966 (s), 876 (w), 808 (w), 780 (w), 748 (m). ^1H NMR (benzene-d_6, 399.6 MHz, 20 °C): δ 1.70 (m, 4H, PCH_2), −8.88 (br d, $^2J_{HP}$(trans) = 153 Hz, 2H; Ir(*H*)), −12.09 (t, $^2J_{HP}$(cis) = 21 Hz, 1H; Ir(*H*)). ^{31}P NMR (benzene-d_6, 161.7 MHz, 20 °C): δ 68.90 (m). ^{19}F

(25) (a) *Chemistry of the Platinum Group Metals*; Hartley, F. R., Ed.; Elsevier: New York, 1991; Chapters 13 and 14. (b) Dickson, R. S. *Homogeneous Catalysis with Compounds of Rhodium and Iridium*; D. Reidel: Dordrecht, Holland, 1985.

NMR (acetone-d_6, 376.05 MHz, 20 °C): δ −75.5, −77.0 (s, PCF_2CF_3), −109 to −113 (overlapping ABX multiplets, PCF_2-CF_3).

Crystal Data for (dfepe)$_2$Ir$_2$(μ-H)$_3$H (3). X-ray data were collected at −100 °C on a Siemens R3m/V automated diffractometer system using Mo Kα radiation. Crystal, data collection, and refinement parameters are summarized in Table 1. All computations used the SHELXTL/IRIS (version 4.2) program library (Siemens Corp., Madison, WI).[26] A red prism of **3** was grown from a saturated hexane solution. Monoclinic unit cell dimensions were derived from a least-squares fit of 47 random reflections (18° < 2θ < 25°). Data were collected using the Wyckoff scan technique with a variable scan rate of 4.0−30.0°/min. Three standard reflections monitored after every 100 data collected showed no systematic variation; the residual for averaging 241 redundant data was 7.15%. Data were not corrected for absorption. $P2_1/n$ space group symmetry was deduced from a statistical analysis of all collected data.

An initial structure solution for **3** was obtained using the SHELXTL direct methods program, which revealed the iridium and phosphorus atoms. All other non-hydrogen atoms were located from a series of difference Fourier maps. Despite data collection at −100 °C, isotropic thermal parameters for a majority of the lighter atoms were excessively large and prevented a satisfactory refinement of the perfluoroethyl groups and both chelate backbones. Accordingly, a refinement model with constrained P−C (1.90 Å), C−C (1.54 Å), and C−F (1.36 Å (CF_2 groups), 1.33 Å (CF_3 groups)) bond distances was adopted. Since four of the eight C_2F_5 groups exhibited significant angular distortions, tetrahedral constraints were subsequently applied to all perfluoroethyl groups. All CF_2 and CF_3 groups were refined using common isotropic thermal parameters, with U(F) values set to 1.2 times that of the associated carbon. Chelate backbone hydrogens were added in idealized positions (d(C−H) = 0.96 Å) with isotropic thermal parameters set to approximately 1.2 times the value of the associated methylene carbon. Hydride ligands were not included in the refinement. *Although these constraints introduce bias into the model, only minor changes in the basic Ir_2P_4 framework were observed.* Full-matrix least-squares refinement gave an R value of 12.10% (R_w = 15.18%) for 3041 data with $F > 4\sigma(F)$. The final difference Fourier map showed residual peaks of 2.42 and −1.80 e/Å^3 associated with the C_2F_5 groups.

Crystal Structure of [(dfepe)Ir(μ-H)(H)$_2$]$_2$ (5). X-ray data were collected at −100 °C as described above and are summarized in Table 1. A suitable light yellow prism of **5** was grown by the slow hydrogenation of **4** in cyclohexane at 3 °C under 2 atm of H_2. Orthorhombic unit cell dimensions were derived from a least-squares fit of 43 random reflections (17° < 2θ < 28°). Data were collected using the Wyckoff scan technique with a variable scan rate of 4.0−30.0°/min. Three standard reflections monitored after every 100 data collected showed no systematic variation. Data were corrected for absorption using an empirical ellipsoidal model based on 360° ψ scans for 12 reflections with 10° < 2θ < 35°. *Pbca* space group symmetry was deduced from a statistical analysis of all collected data.

(26) Sheldrick, G. Siemens XRD, Madison, WI.

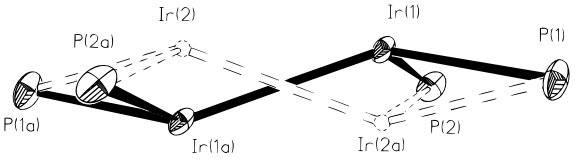

Figure 4. Core molecular structure of **5**, showing the approximate 2-fold disorder between the alternative iridium atom sites Ir(1) (SOF = 0.84) and Ir(2) (SOF = 0.16).

The structure of **5** was solved using direct methods, which placed the dimeric molecule on a crystallographic inversion center relating the two (dfepe)Ir units. After all the non-hydrogen atoms were located and refined isotropically, difference Fourier maps revealed a substantial electron density peak (approximately 19 e$^-$) 0.92 Å from the Ir(1) center. The R factor at this point was 13%. This residual density was satisfactorily modeled as an additional iridium position Ir(2) (refined site occupation factor 0.1609) with Ir−Ir and Ir−P distances essentially identical with those found for Ir(1). These two alternative iridium positions are approximately related by a 2-fold rotation normal to the plane defined by Ir(1) and Ir(2) atoms and their symmetry-related equivalents (see Figure 4). The effects of iridium positional disorder were not reflected by any corresponding anomalies in the phosphorus atom refinements but instead were confined primarily to distortions in two of the perfluoroethyl dfepe substituents, C(5)−C(6) and C(7)−C(8). Distance constraints to P(1)−C(5) and P(2)−C(7) (1.90 Å), C(5)−C(6) and C(7)−C(8) (1.54 Å), C(5)−F(6), C(7)−F(11), and C(7)−F(12) (1.36 Å), and C(8)−F(13), C(8)−F(14), and C(8)−C(15) (1.33 Å) were applied which did not result in any significant changes in the heavy atom metrical data. All non-hydrogen atoms were refined anisotropically. Chelate backbone hydrogen atom positions were added in ideal calculated positions with d(C−H) = 0.96 Å with fixed isotropic thermal parameters set at 1.2−1.3 times the isotropic equivalent of the attached carbon atom. Hydride atom positions were not located on difference Fourier maps and were not included in the final structure model. Full-matrix least-squares refinement gave an R value of 7.16% (R_w = 7.31%) for 2278 data with $I > 2\sigma(I)$. The final difference Fourier map showed residual peaks of 3.31 and −3.88 e/Å^3 associated with the Ir(1) atom.

Acknowledgment. We thank Profs. R. H. Morris and R. Eisenberg for helpful discussions. This work has been supported by the National Science Foundation (Grant No. CHE-9310550). Johnson Matthey is also gratefully acknowledged for a generous loan of iridium and rhodium chlorides.

Supporting Information Available: Tables giving X-ray crystallographic data for **3** and **5**, including structure determination summaries, bond lengths and angles, anisotropic displacement coefficients, and atom coordinates and isotropic displacement coefficients (18 pages). Ordering information is given on any current masthead page.

OM950722C

Downloaded by CARLI CONSORTIUM on June 30, 2009
Published on January 23, 1996 on http://pubs.acs.org | doi: 10.1021/om950722c